

Strong Confinement and Oscillations in Two-Component Bose-Einstein Condensates

Q-Han Park^{1,2} and J. H. Eberly¹

¹ Rochester Theory Center for Optical Science and Engineering and
Department of Physics and Astronomy,
University of Rochester, Rochester, New York 14627-0171

² Department of Physics, Kyunghee University, Seoul, 130-701, Korea
(November 6, 2018)

Abstract: We present a new model of BEC dynamics based on strong confinement near the ground state. The model predicts oscillations in a two-component condensate, based on interference of non-spreading wave packets moving within a pair of tilted nearly square potentials. The oscillations are similar to those recently reported for a magnetically trapped ⁸⁷Rb condensate, and the model's predictions give good quantitative agreement with the experiments.

03.75.Fi, 67.90.+z, 67.57.Fg, 42.50.Md

Since its first application to quantum Rabi oscillations in the two-level cavity QED context, collapse and revival analysis [1] has been used for the understanding of a widening class of recurrent physical phenomena. The timing and nature of revivals have been employed in interpreting the dynamics of a variety of quantum systems [2,3], but a number of cases provide puzzling features that are considered open questions [4].

Recent elegant experimental observations of Rabi-type oscillations in a two-component Bose-Einstein condensate of ⁸⁷Rb [5] offer a new example that has resisted analysis. Multi-component BEC's [6,7] in the presence of external driving fields have provided a rich spectrum of physical responses to challenge current theoretical understanding. In the two-component case of interest here [8,9] the theoretical situation has been described by various groups [9,10]. In particular, differential shifting of the trap centers for two species has led to interesting theoretical predictions such as a "condensate dressed state" [11], Josephson-type oscillations and periodic modulation of Rabi oscillations [12], all of which originate in analogies with two-level quantum optical systems. Despite heuristic arguments using "twists" of an $SU(2)$ order parameter [5], it is fair to say that the fundamental dynamics of the observed oscillations are not understood.

In this Letter, we go beyond revival analysis to present a new quantum mechanical picture of the physics based on a strong confinement model, which explains experimentally observed features quite well. We show that the coupled Gross-Pitaevski (GP) equations for the two-component Bose-Einstein condensate can be decoupled by a time-dependent dressing transformation. The transformed Schrödinger equations describe local-

ized wavepackets that accelerate in opposite directions and bounce back and interfere after hitting the walls of the confinement. We find that the spatial and temporal behavior of the two BEC's are determined by these wavepackets and the experimental observations that have been reported can be explained in detail in terms of their interference. Our model gives quantitative predictions that also agree well with numerical simulation of the coupled GP equations.

The two components of the condensate, ψ_1 and ψ_2 , obey GP equations that are coupled to each other via the "drive" parameter Ω , which plays a role similar to the Rabi frequency of a driven two-level system:

$$i\frac{\partial\psi_1}{\partial t} = H_0\psi_1 + \mu(r_1|\psi_1|^2 + |\psi_2|^2)\psi_1 + \frac{\delta}{2}\psi_1 + \frac{\Omega}{2}\psi_2 \quad (1)$$

$$i\frac{\partial\psi_2}{\partial t} = H_0\psi_2 + \mu(|\psi_1|^2 + r_2|\psi_2|^2)\psi_2 - \frac{\delta}{2}\psi_2 + \frac{\Omega}{2}\psi_1, \quad (2)$$

where $H_0 \equiv -\frac{1}{2}\frac{\partial^2}{\partial z^2} + \frac{1}{2}z^2$ is the bare Hamiltonian for the harmonic trap. For simplicity we present here only a one dimensional model. We have used the axial oscillation frequency ω_z to express units: $\hbar\omega_z$ is our unit of energy and $1/\omega_z$ and $d_z = \sqrt{\hbar/m\omega_z}$ are the units of time and distance. The coefficient $\mu = 4\pi a_{12}N/d_z$ measures the strength of interaction between two species of BEC where N is the total particle number and a_{12} is the interspecies scattering length. The small difference reported [5] for the ratios in ⁸⁷Rb, $r_1 = a_1/a_{12} \approx 1.03$ and $r_2 = a_2/a_{12} \approx 0.97$, among scattering lengths has little effect on the subsequent discussion so we assume that $r_1 = r_2 = 1$ in the following.

The detuning δ and the interspecies coupling Ω , both measured in the unit ω_z , can depend on the axial position z . We will make assumptions of no detuning ($\delta = 0$) and a linear z -dependence of coupling: $\Omega = \Omega_0 + 2\beta z$, consistent with experiment [5]. The nonvanishing detuning case will be discussed later. Now we introduce the time-dependent dressing transformation

$$\phi_{\pm} \equiv (\psi_1 \pm \psi_2)e^{\pm i\Omega_0 t/2}, \quad (3)$$

which gives two decoupled GP equations in a slow time frame:

$$i\frac{\partial\phi_{\pm}}{\partial t} = -\frac{1}{2}\frac{\partial^2\phi_{\pm}}{\partial z^2} + V_{\pm}\phi_{\pm}, \quad (4)$$

where the potentials V_{\pm} are given by

$$V_{\pm}(z) = \frac{1}{2}z^2 + \frac{\mu}{2}(|\phi_{+}|^2 + |\phi_{-}|^2) \pm \beta z. \quad (5)$$

The first crucial observation is that although these potentials are spatially very nonlinear, they are nearly independent of time if the system is started near its ground state. This is due to the strong and relatively tight nonharmonic confinement provided in the present case by the GP interaction. In principle, the potentials depend on time through the total density of the condensate, $\rho_{tot} = |\psi_1|^2 + |\psi_2|^2 = \frac{1}{2}(|\phi_{+}|^2 + |\phi_{-}|^2)$, but ρ_{tot} changes very little during hundreds of Rabi cycles that are well-resolved in the experiments. This is evident in the relatively very rigid spatial shape of the total condensate density seen in the series of snapshots in Fig. 1. To obtain the snapshots we solved the coupled GP equations using the combined split-step Fourier technique familiar from fiber optics theory (where the GP equation is called the non-linear Schrödinger equation), modified to include two components [13]

The second crucial observation, also evident in Fig. 1 and noted previously [8], is that ρ_{tot} maintains a Thomas-Fermi-like spatial distribution. We have found that this allows the confining forces on the packets to be converted into boundary conditions, leaving relatively free ϕ_{\pm} packets to accelerate slowly in opposite directions at the rate $\pm\beta$ along the bottoms of two potential wells that are nearly square but tipped in opposite directions, as shown in Fig. 2. We will now demonstrate that this simplified picture is powerfully effective in unraveling relatively complicated condensate evolution.

If, as in the JILA experiments, a condensate at nearly zero temperature is prepared initially in the pure 1 component, i.e. $\psi_1(z, 0) = \psi_g(z)$, $\psi_2(z, 0) = 0$, we have equally distributed ϕ 's : $\phi_{+}(z, 0) = \phi_{-}(z, 0) = \psi_g(z)$. As these \pm probability packets fall along the bottom of the well toward opposite walls they must interfere since ϕ_{+} and ϕ_{-} are coherent parts of the same two-component condensate. An effective interaction between the decoupled \pm packets comes from their interference to produce the observed density $|\psi_1|^2$:

$$\begin{aligned} |\psi_1|^2 &= \frac{1}{4}(|\phi_{+}|^2 + |\phi_{-}|^2) + \frac{1}{2}\Re(e^{i\Omega_0 t}\phi_{+}^*\phi_{-}) \\ &\approx \frac{1}{2}|\psi_g|^2 + \frac{1}{2}\Re(e^{i\Omega_0 t}\phi_{+}^*\phi_{-}), \end{aligned} \quad (6)$$

where \Re denotes the real part.

First we show additional results of direct numerical integration of the original two nonlinear GP equations (4). The calculated temporal evolution of the space-integrated population of component 1 is shown in Fig. 3. The corresponding experimental data is given in Fig.

4-a. Rapid oscillations at the drive frequency Ω_0 are evident, as the population cycles between components 1 and 2. An apparent collapse in region *A*, and a revival or perhaps a pair of them, is seen in regions *D* and *E*. Small features at *B* and *C* are also noted. Now we will use the strong confinement model to obtain a detailed understanding of the curve. As we will see, revivals in the conventional sense play no role. The correct explanation is in some respects simpler, and capable of wider applicability as we mention at the end.

Now we return to our simplified picture, according to which the main slow motion is acceleration with each packet moving toward an opposite wall. This main slow motion can also be factored out of the quantum amplitudes by defining

$$\chi_{\pm}(z, t) = \phi_{\pm}(z, t) \exp(\pm i\beta z t + i\beta^2 t^3/6), \quad (7)$$

and changing the coordinates into those of the two accelerating frames: $T = t$, $Z_{\pm} = z \pm \beta t^2/2$. The packets χ_{\pm} satisfy the free Schrödinger equation, $(i\partial/\partial T + \frac{1}{2}\partial^2/\partial Z_{\pm}^2)\chi_{\pm} = 0$, with initial conditions $\chi_{\pm}(T = 0) = \psi_g$, and so can be integrated directly to yield

$$\chi_{\pm} = \frac{1}{2\pi} \iint dz' dk e^{ik(z-z' \pm \beta t^2/2) - ik^2 t/2} \psi_g(z', 0). \quad (8)$$

Since the initial ψ_g is very smooth, this shows that the two χ_{\pm} move apart with a combined quantum mechanical dispersion which is relatively small in our Thomas-Fermi like configuration. The interference term in Eq.(6) is now given by $\frac{1}{2}\Re(\exp[i\Omega_0 t + 2i\beta z t]\chi_{+}^*\chi_{-})$ with χ_{\pm} as given above.

Thus we predict spatial oscillations with wavelength $L_0 = \pi/\beta t$ to develop in the population of condensate 1, dramatically evident in Fig. 1-B. The interference occurs in the region where the \pm packets continue to overlap, a shrinking region of length $L = 2R - \beta t^2$, where the full axial length is $2R$. These spatial interference oscillations have nodes that can be monitored experimentally [see Fig. 4-b] and the node formation has been called “twisting.” Various effects are predicted and labeled in Fig. 3 as follows.

A. Collapse. The number of nodes in existence at time t is fixed at $n = L/L_0 = \beta t(2R - \beta t^2)/\pi$. By about the time of the second twist there is a good balance of the two components in the condensate (e.g., $|\psi_1|^2 \approx |\psi_2|^2 \approx 0.5$), which shows up in the data as the completion of the “collapse” at the end of region *A* in Fig. 3. From $n = 2$, with the parameters used in the calculation ($R = 8.53$, $\beta = 0.25$), one easily finds for the collapse time $t_C \approx 1.5$, in excellent agreement with Fig. 3.

B. Twist resolvability. Our formula also predicts a maximum twist number n_M , and says that it occurs at time $t_M = \sqrt{2R/3\beta}$, after which the \pm packets are falling too fast to have resolvable spatial interference. This gives

$n_M = \sqrt{32\beta R^3/27\pi^2}$, or $t_M = 4.77$ and $n_M = 4.3$, also in good agreement with the observed behavior in region B.

C. *Bounce time*, $t = t_B$. When the centers of ϕ_{\pm} reach the walls at time $t_B = \sqrt{2R/\beta}$ ($= 8.26$ in our case), the ϕ_{\pm} become maximally separated and have a finite but minimally overlapping interference region. Eq. (6) shows that in the near-wall regions, the densities $|\psi_1|^2$ and $|\psi_2|^2$ reduce to about half of the initial ground state density. This cannot be seen in Fig. 3, but is confirmed by examining snapshots of the spatial behavior of the two condensate components. Five such snapshots were already given in Fig. 1, and Fig. 1-C confirms that at the time of the wall bounce, in the regions near the walls, the two components are not interfering but each contain about half of the total density. Of course, due to reflection at the wall and subsequent self-interference, there arise complicated motions for each ϕ_{\pm} . A more complete analytic description of the interference between ϕ_{\pm} can be made by solving the Schrödinger equation (4) directly in terms of Airy functions.

D. *Packet recovery*, $t = t_R$. After bouncing from the strong confinement, the packets ϕ_{\pm} return approximately to their initial positions. As they return, oscillations in the overlapping region spread out over the half-ground-state density region with increasing amplitude and wavelength. When the number of nodes reaches three, with one central peak and two side peaks, oscillations in the half-ground-state region interfere most destructively, thereby minimizing the population of component 1 (Fig. 1-D). This happens before completing one round trip by the amount of time required to develop three nodes in the initial stage. However, the external coupling drive quickly switches back from the minimum population to the maximum population for condensate 1. Thus, the maximal recovery occurs at $t_R = 2t_B - \Delta t$ where Δt is obtained from $\beta\Delta t(2R - \beta(\Delta t)^2)/\pi = 3$.

In our case, $\Delta t = 2.4$ and $t_R = 14.1$. This shows that the maximum revival of population does not come with the original shape. In fact, Fig. 1-D shows that it rather has the shape of a dark soliton. This is also in agreement with the reduced contrast of about 60 percent of the original.

E. *Completing one cycle*, $t = t_F$. At the classical return time, $t_F = 2t_B$, the recovery of population of condensate 1 happens but in a smaller scale than in case D, as shown in Fig. 1-E.

In closing, let us return to an earlier point. In the spin-boson language of revival analysis, a vanishing detuning ($\delta = 0$ in the evolution equation (2), for example) corresponds to exactly zero Zeeman splitting of the two spin states, removing any possibility of resonant coincidence with the boson (oscillator) transition frequencies. This is why revival analysis is misapplied to the existing data. However, although the BEC oscillator is very anharmonic under its strong confinement, one suspects that

it could support a near-resonance with a non-zero δ , if δ were large enough. In such a case one would have an intriguing combination of bouncing packets and quantum revivals (which themselves are of course known to have packet interpretations). Since the energy spacings in the confinement are small, δ would not have to be very large.

In this Letter, we have introduced a quantum mechanical packet model which provides an excellent qualitative description of the previously unexplained temporal behavior of oscillations in two-component driven-BEC experiments. One clearly sees that the strong-confinement bouncing packet model permits easy analysis that predicts all five distinct events in the temporal record as well as predicting their appropriate time scales. Figs. 1-3 compare these events with numerical simulations and with the experimental record in Fig. 4.

It is clear that this model is not restricted to the two-component case, and it will be interesting to extend our work to the three-component BEC recently reported [7] and partially analysed [14].

We thank S. Raghavan for his participation in the early stage of this work and C.R. Stroud, Jr. for a key remark about Airy packets. This research is supported by NSF grant PHY94-15583. Q.P. is also supported in part by the Brain Korea 21 Project, and by KOSEF 97-07-02-02-01-3.

-
- [1] J.H. Eberly, N.B. Narozhny and J.J. Sanchez-Mondragon, Phys. Rev. Lett. **44**, 1323 (1980), and H.I. Yoo and J.H. Eberly, Phys. Reports **118**, 239 (1985)
 - [2] J. Parker and C.R. Stroud, Jr., Phys. Rev. Lett. **56**, 716 (1986), G. Rempe, H. Walther and N.Klein, Phys. Rev. Lett. **58**, 353 (1987), I. Averbuch and N.F. Perelman, Phys. Lett. **A139**, 449 (1989), and J.A. Yeazell, M. Mallalieu and C.R. Stroud, Jr., Phys. Rev. Lett. **64**, 2007 (1990).
 - [3] D.M. Meekhof *et al.*, Phys. Rev. Lett. **76**, 1796 (1996), M. Brune *et al.*, Phys. Rev. Lett. **76**, 1800 (1996).
 - [4] See, for example, S.C. Guo, Phys. Rev. A **40**, 5116 (1989), C.C. Gerry and J.H. Eberly, Phys. Rev. A **42**, 6805 (1990), and D.A. Cardimona, *et al.*, Phys. Rev. A **43**, 3710 (1991).
 - [5] M. R. Matthews *et al.*, Phys. Rev. Lett. **83**, 3358 (1999).
 - [6] C. J. Myatt *et al.*, Phys. Rev. Lett. **78**, 586 (1997).
 - [7] J. Stenger *et al.*, Nature (London) **396**, 345 (1998).
 - [8] D. S. Hall *et al.*, Phys. Rev. Lett. **81**, 1539 (1998).
 - [9] D. S. Hall, M. R. Matthews, C. E. Wieman, and E. A. Cornell, Phys. Rev. Lett. **81**, 1543 (1998).
 - [10] R. Dum, J. I. Cirac, M. Lewenstein, and P. Zoller, Phys. Rev. Lett. **80**, 2972 (1998); R. J. Ballagh, K. Burnett, and T. F. Scott, Phys. Rev. Lett. **78**, 1607 (1997); K.-P. Marzlin, W. Zhang, and E. M. Wright, Phys. Rev. Lett. **79**, 4728 (1997); and

J. Williams *et al.*, Phys. Rev. A **57**, 2030 (1998).

- [11] P. B. Blakie, R. J. Ballagh, and C. W. Gardiner, cond-mat/9902110.
 [12] J. Williams *et al.*, Phys. Rev. A **59**, R31 (1999); and cond-mat/9904399.
 [13] See, for example, G.P. Agrawal, *Nonlinear fiber optics*, Academic Press (Orlando, 1999). In the numerical calculation we have chosen these parameter values, $\beta = 0.25$, $\mu = 414$, $\Omega_0 = 28.85$, in accordance with the experiment [5].
 [14] H. Pu, *et al.*, Phys. Rev. A **60**, 1463 (1999)

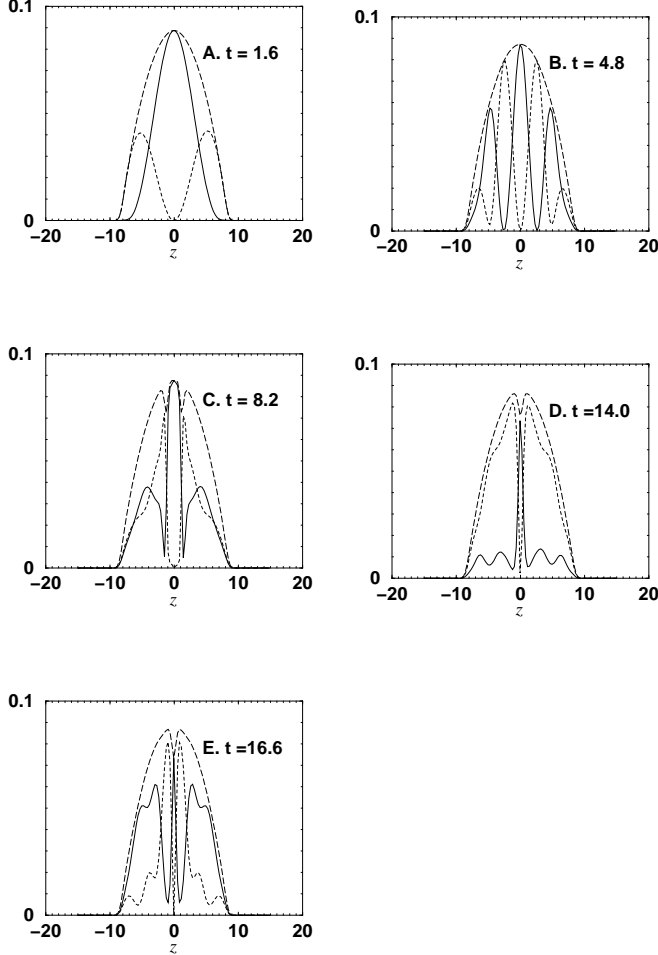


FIG. 1. Calculated density profiles of condensates at five distinct times that are the keynote instants during evolution noted in Fig. 3. Solid and dotted lines represent condensates 1 and 2, and the dashed line represents the total density ρ_{tot} . Note the strong time-independence of ρ_{tot} .

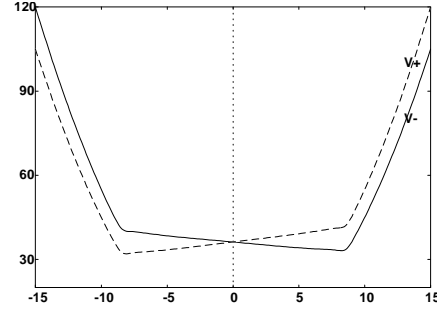


FIG. 2. Potentials V_{\pm} . Since the total density maintains the Thomas-Fermi shape, the potentials have a flat bottom while the wall is the upper portion of a harmonic potential.

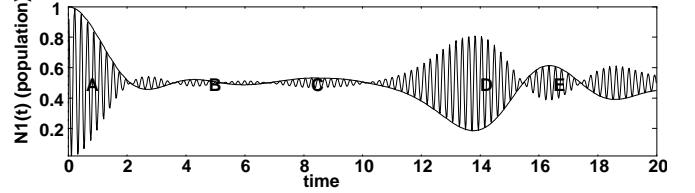


FIG. 3. Plot of the population of condensate 1. The thick line represents the case with no constant coupling drive ($\Omega_0 = 0$) while the fast oscillating thin line represents the case with $\Omega_0 = 28.85$. Five distinct events are specified at the calculated times, which are described separately in the text.

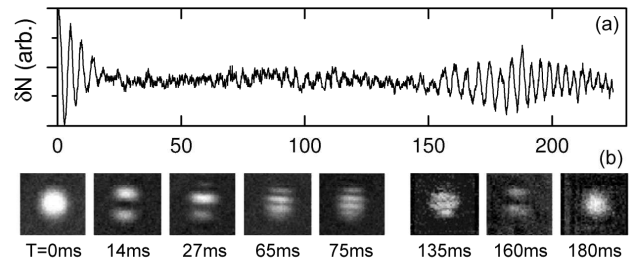


FIG. 4. Experimental data from ref. [5]. The modest discrepancy in time registry copared to Fig. 3 is due to our simplified 1D modeling and also to an experimental departure from $\delta = 0$, evident because the mid-line in part 4(a) shows a component 1 fraction lower than 50%.